

Identification and validation of DLX4 as a prognostic and diagnostic biomarker for clear cell renal cell carcinoma

JIAWEI WANG^{1*}, LIANGJUN TAO^{2,3*}, YINGQING LIU¹, HEQIAN LIU¹,
XUDONG SHEN¹ and LINGSONG TAO¹

¹Department of Urology, The Second People's Hospital of Wuhu, Wuhu, Anhui 241000;

²Department of Urology, The First Affiliated Hospital of Anhui Medical University;

³Anhui Province Key Laboratory of Genitourinary Diseases, Anhui Medical University, Hefei, Anhui 230022, P.R. China

Received July 18, 2021; Accepted November 9, 2021

DOI: 10.3892/ol.2023.13732

Abstract. Clear cell renal cell carcinoma (ccRCC) is a lethal cancer, and biomarkers for exact diagnosis and predicting prognosis are urgently needed. The present study aimed to determine the roles of distal-less homeobox (DLX) family genes in ccRCC. The clinicopathological and mRNA expression data of patients with ccRCC were derived from The Cancer Genome Atlas database. Kaplan-Meier curves, univariate and multivariate Cox hazard analyses, in addition to receiver operator characteristic curves were used to evaluate the prognostic and diagnostic values. A single-sample gene set enrichment analysis was used to quantify the infiltration levels of immune cells. Reverse transcription-quantitative polymerase chain reaction (RT-qPCR) and immunohistochemistry were conducted to examine the expression levels of DLX4 in tumor and adjacent tissue; the results demonstrated that DLX4 was highly expressed in ccRCC tissues compared with normal renal tissues. Furthermore, DLX4 expression was associated with tumor stage and grade. High proportions of males, advanced pathological stage, higher tumor grade and T, N and M stage were also observed in the high DLX4 expression group. Patients with the high DLX4 expression levels tended to have lower overall survival and disease-free survival rates compared with those with low DLX4 expression. DLX4 expression also showed favorable diagnostic efficiency in ccRCC patients. Based on functional enrichment analysis, cell cycle related pathways, epithelial-mesenchymal transition, glycolysis and inflammatory response were associated with the expression levels of DLX4. Furthermore, DLX4 expression

was revealed to be associated with tumor immunosuppressive microenvironment. Overall, the expression level of DLX4 may be considered a novel prognostic indicator in ccRCC and a specific diagnostic biomarker for patients with ccRCC.

Introduction

Renal cell carcinoma (RCC) is one of the most common malignancies among adults and is estimated to have caused 73,750 new cases and 14,830 deaths in the United States in 2020 (1). Clear cell (cc)RCC is the most common histologic subtype of RCC, accounting for ~90% of RCC cases (2). ccRCC is the leading cause of death in the majority of patients with RCC and is responsible for ~3% of all adults diagnosed with cancer (3). The morbidity and mortality of ccRCC are also increasing in the majority of countries (4). Despite remarkable advances in the diagnosis and treatment of ccRCC in recent years, ccRCC remains one of the deadliest cancers. In fact, metastasis at diagnosis occurs in a large proportion of patients owing to the lack of characteristic clinical symptoms (5). Approximately 30% of patients with ccRCC developed recurrence and progression despite surgical resection of the primary tumor (6,7). ccRCC is a chemo- and radioresistant neoplasia, with limited alternative treatment options available for therapeutic use (8). At present, novel therapeutic options for ccRCC include anti-angiogenic agents (such as sorafenib, sunitinib, pazopanib, axitinib and bevacizumab), mTOR inhibitors (temsirolimus and everolimus) and immune checkpoint inhibitors (nivolumab) (9,10). However, these drugs result in only partial responses in few patients with ccRCC and a poor prognosis. Therefore, there is an urgent need to identify new biomarkers for accurate diagnosis of ccRCC and to explore its underlying mechanisms.

The distal-less homeobox (DLX) gene family is a cluster of homeobox genes comprising six different members (DLX1-DLX6) (11). DLX is postulated to serve a role in forebrain and craniofacial development. In fact, according to previous studies, the DLX gene family may be involved in early development and cell differentiation, and is frequently dysregulated in neoplasms (12,13). For instance, DLX1 may promote progression and metastasis of prostate and ovarian cancer by enhancing TGF- β /SMAD4 signaling (14,15). DLX2 could counteract TGF- β -induced cell cycle arrest and apoptosis to

Correspondence to: Dr Lingsong Tao, Department of Urology, The Second People's Hospital of Wuhu, 259 JiuHuaShan Avenue, Wuhu, Anhui 241000, P.R. China
E-mail: taolingsong@sina.com

*Contributed equally

Key words: clear cell renal cell carcinoma, biomarker, prognosis, diagnosis

promote tumorigenesis (16), and it is considered to be a marker of survival and disease progression in prostate cancer (17); DLX3 regulates cell cycle progression and squamous tumor growth (18). DLX5 is involved in the growth and diffuse spreading of invasive glioma cells (19), and DLX4 serves a vital role in the early development and differentiation of tumor cells (12). DLX4 may induce a megakaryocytic transcriptional program by inducing IL-1 β and NF- κ B signaling (20). DLX4 may induce expression of the cell surface molecule CD44 in ovarian tumor cells by stimulating IL-1 β -mediated NF- κ B activity, thereby promoting tumor-mesothelial cell interactions and peritoneal metastasis of ovarian cancer (21). Chen *et al* (22) adapted the approach of network-based molecular modeling of physiological behaviors to specifically isolate physiological behaviors in alopecia areata model that contribute to the recruitment of immune cells in autoimmune disease. They found that DLX4 is expressed in the skin and could induce recruitment of immune cells in alopecia areata model. Therefore, they propose that DLX4 is a master regulator of immune infiltration recruitment, and the loss of DLX4 expression may contribute to immune evasion in cancer. These studies suggested that aberrant expression of DLX gene family may be related to the development and metastasis of tumors. However, the roles of DLX gene family in ccRCC patients remain unclear.

In the present study, the expression levels of DLX gene family in ccRCC were examined and its prognostic value and correlations with pathological parameters were evaluated. Here, differences in both overall survival and disease-free survival (DFS) were selected to investigate the association with the distributions of clinical phenotypes. DLX4 was selected for further validation and its potential functional mechanisms were explored.

Materials and methods

Data acquisition. mRNA expression data of six members of DLX gene family in The Cancer Genome Atlas (TCGA) dataset (HTSeq Counts) were acquired from University of California, Santa Cruz (UCSC) Xena website (xenabrowser.net) (23); the project number was TCGA-KIRC. The data were processed using RSEM normalization methods and expressed as $\log_2(x+1)$ transformed. Clinical information of 533 patients, including age, sex, pathological stage, pathological grade, TNM stage, overall survival and survival status were obtained from UCSC Xena. DFS of patients with ccRCC was obtained from the cBio Cancer Genomics Portal (<http://cbioportal.org>).

Differential expression levels, diagnostic efficiency and prognostic significances. The differential expression of six members of the DLX gene family was compared between ccRCC and adjacent normal renal tissues in TCGA dataset. The differential expression of DLX4 was also compared between the different clinical subgroups (advanced vs. early stage, high vs. low grade, N0 vs. N1, M0 vs. M1). Kaplan-Meier curves and log-rank tests were performed to evaluate the prognostic significance, and receiver operating characteristic (ROC) curves were generated to assess the diagnostic efficiency (24). Univariate and multivariate Cox hazard analyses were

performed to assess the overall survival and DFS of patients with ccRCC.

ccRCC tissue samples. A total of 40 pairs of ccRCC tumors and matched normal renal tissues were retrieved from the Department of Urology at the Second People's Hospital of Wuhu (Wuhu, China) and The First Affiliated Hospital of Anhui Medical University (Hefei, China) between May 2019 and May 2020. Adjacent normal renal tissues, ≥ 2 cm away from the location of the tumor, were cut and collected. Samples were placed in RNAlater stabilization solution (Invitrogen; Thermo Fisher Scientific, Inc.) and frozen in liquid nitrogen. These samples were evaluated by two pathologists to confirm the histopathological results of ccRCC. Inclusion criteria were ccRCC, and exclusion criteria were other types of RCC and benign renal tumors. Written informed consent was provided by all patients. The present study was approved by the Ethics Committee of Human Research of The Second People's Hospital of Wuhu and The First Affiliated Hospital of Anhui Medical University (approval no. PJ2019-14-22). The study methodology conformed with the standards of the Declaration of Helsinki.

RNA extraction and reverse transcription-quantitative polymerase chain reaction (RT-qPCR). Total RNA was extracted from ccRCC tissue using the TRIzol[®] (Invitrogen; Thermo Fisher Scientific, Inc.) method. The purity and concentration of total RNA solution were detected using a NanoDrop spectrophotometer (NanoDrop Technologies; Thermo Fisher Scientific, Inc.). Extracted RNA was reverse transcribed into cDNA using a PrimeScript[™] RT with gDNA Eraser kit (Takara Bio, Inc.) according to the manufacturer's protocol. The cDNA was subjected to qPCR by a SYBR Green Mix (Takara Bio, Inc.). Thermocycling conditions were as follows: Initial denaturation at 95 for 30 sec, followed by 40 cycles of 95°C for 5 sec and 60°C for 34 sec, then final extension at 95°C for 15 sec, 60°C for 1 min and 95°C for 15 sec. A final reaction volume of 20 μ l was used, and the ABI 7500 Real-Time PCR System (Thermo Fisher Scientific, Inc.) was used to measure the reactions. Relative gene expression of DLX4 were analyzed using the $2^{-\Delta\Delta C_q}$ method (25). GAPDH was used as endogenous control to normalize the relative expression of DLX4. The primers were purchased from Sangon Biotech Co., Ltd., and the sequences were as follows: DLX4 forward, 5'-CAGCACCTAAACCAGCGTTTC-3' and reverse, 5'-GAGCTTCTTATACCTGGAGCGTT-3'; and GAPDH forward, 5'-GGGAGCCAAAAGGGTCAT-3' and reverse, 5'-GAGTCCTTCACGATACCAA-3'.

Immunohistochemistry. Paraffin-embedded tissue specimens were sliced into 4- μ m-thick sections. The slides were placed in a 60°C thermostat and baked for 20 min to dewax. Then, the slides were hydrated in xylene I (30 min), xylene II (30 min), anhydrous ethanol (5 min) twice and 95, 90, 80 and 70% ethanol (5 min each). Then, the slides were heated at 100°C for 10 min in citric acid buffer (0.01 M, pH 6.0) for antigen retrieval. The slides were incubated in 3% hydrogen peroxide solution (cat. no. SP 9000; Beijing Zhongshan Jinqiao Biotechnology Co., Ltd.) for 15 min at room temperature and washed three

times in phosphate-buffered saline (PBS; pH 7.4). The slides were blocked with 3% bovine serum albumin (cat. no. G5001; Servicebio) for 1 h at room temperature, then incubated with anti-DLX4 antibody (1:100; cat. no. DF3387; Affinity Biosciences, Ltd.) overnight at 4°C. After three washes with PBS, the slides were incubated with biotinylated goat anti-rabbit IgG (1:200; cat. no. G23303; Servicebio) for 2 h at room temperature. Finally, DAB (Beyotime Institute of Biotechnology) was used to detect the immune complexes and the sections were counterstained with hematoxylin for 3 min at room temperature. The images were captured using a light microscope (Olympus Corporation). DLX4 expression was measured based on the intensity of immune staining (intensity score) with ImageJ version 6.0 software (National Institutes of Health), as previously described (26).

Gene set enrichment analysis (GSEA). Patients in TCGA data set were divided into high and low expression groups according to the median values of DLX4 gene expression. GSEA was conducted to explore the possible functional mechanisms of DLX4 in ccRCC with GSEA 3.0 software (Broad Institute; broad.mit.edu/gsea) (27). The reference gene set file was h.all.v7.0.symbols.gmt; normalized P-value <0.05 and FDR <0.25 were set as threshold values.

Functional enrichment analysis. Pearson correlation coefficients was calculated to determine the association between DLX4 gene expression and genes in TCGA dataset. Genes that strongly correlated with the expression levels of DLX4 (correlation coefficient $R > 0.4$) were obtained as previously described (28). A total of 559 positively correlated genes and 226 negatively correlated genes were identified. Kyoto Encyclopedia of Genes and Genomes (KEGG) and Gene Ontology (GO) enrichment analyses were performed using The Database for Annotation, Visualization and Integrated Discovery (<https://david.ncifcrf.gov>) to investigate the possible molecular mechanisms of these selected genes. The cutoff value was set at $P < 0.05$.

Estimation of the immune microenvironment composition. To quantify the cellular composition of the immune infiltrates in each patient in TCGA dataset, a set of metagenes, including non-overlapping sets of genes that are representative of 28 specific immune cell subpopulations, was obtained from a previous study (29). Subsequently, single-sample GSEA was used to quantify the 28 types of immune cells based on the metagenes. In the tumor microenvironment, immune and stromal cells are the two main non-tumor components; these components have been proposed to be valuable for tumor treatment and prognosis (30). To assess the tumor microenvironment associated with DLX4 expression levels, the immune and the stromal scores (which reflect the infiltration levels of non-tumor cells) for the TCGA dataset were calculated using the ESTIMATE package (30). The differences in immune cell composition and immune and stromal scores were compared between the high and low DLX4 expression groups, which were divided based on the median expression values. In addition, the correlations between DLX4 expression levels and immunosuppressive immune cells were evaluated.

Comparison of tumor mutation burden and cytolytic activity. Tumor mutation burden (TMB) is defined as the total amount of coding errors of somatic genes, base substitutions, insertions or deletions detected per million bases (31). In the present study, 38 megabases was used as the exon length. TMB was calculated as (the number of variants)/(exon length) for each patient with ccRCC using Perl scripts (32). The somatic mutation status data of ccRCC samples (workflow type: VarScan2 Variant Aggregation and Masking) were downloaded from the TCGA data portal (<https://portal.gdc.cancer.gov/repository>) in May 2021. The cytolytic activity scores were calculated as the geometric mean of the granzyme A and perforin expression (13). The TMB scores and cytolytic activity scores were also compared between high and low DLX4 expression groups.

Statistical analysis. For equivalent variables with a normal distribution, an unpaired Student's t-test was performed for comparisons between the two groups, and one-way ANOVA followed by Tukey's post hoc test was used for comparison between multiple groups. The paired Student's t-test was used to compare paired samples. For non-normally distributed variables, the Wilcoxon rank-sum test was performed for comparisons between two groups. Pearson's χ^2 test was used to evaluate the distributions of clinical factors between the high and low-DLX4 expression groups. Log-rank tests were used for Kaplan-Meier curves to assess survival differences. The correlations between DLX4 expression and tumor immunosuppressive cells were evaluated using Pearson's correlation analysis, and 'general linear model' method was used to fit curves. $P < 0.05$ was used to indicate a statistically significant difference.

Results

Relative expression of DLX family genes in ccRCC. To investigate the roles of DLX family genes in ccRCC, the mRNA expression levels of six members of the DLX family in the TCGA dataset were investigated. A heat map revealed the overall expression levels of the six members of the DLX family between normal and tumor samples in TCGA dataset (Fig. 1A). Furthermore, the expression levels of six members were compared between normal and tumor samples. Downregulated levels of DLX3 and upregulated levels of DLX1, DLX2, DLX4, DLX5 and DLX6 were observed in tumor samples compared with normal samples in TCGA dataset (Fig. 1B). The expression levels of paired normal and tumor samples in TCGA dataset were also compared, which revealed the same expression patterns (Fig. 1C).

Prognostic values of DLX family in ccRCC. Patients in the TCGA data set were divided into high and low expression group according to the median values of the mRNA expression levels for each gene of the DLX family. A total of 511 patients with ccRCC with overall survival and 422 with DFS information were included. The differences in overall and DFS status for six members of DLX family were compared using the χ^2 test. The distribution for overall survival status was found to be significantly different for DLX2 and DLX4, whereas the distribution for DFS status was significantly different for DLX2, DLX4 and DLX5 (Table I). Kaplan-Meier curves

Table I. Comparison of overall survival and DFS between different expression levels of DLX1-6.

| Variable | Overall survival | | DFS | |
|---------------------|------------------|---------|----------|---------|
| | χ^2 | P-value | χ^2 | P-value |
| DLX1 (high vs. low) | 2.530 | 0.112 | 0.121 | 0.728 |
| DLX2 (high vs. low) | 9.286 | 0.002 | 10.939 | <0.001 |
| DLX3 (high vs. low) | 0.388 | 0.533 | 1.424 | 0.233 |
| DLX4 (high vs. low) | 41.010 | <0.001 | 26.160 | <0.001 |
| DLX5 (high vs. low) | 2.420 | 0.120 | 7.146 | 0.008 |
| DLX6 (high vs. low) | 0.992 | 0.319 | 0.964 | 0.326 |

DFS, disease-free survival; DLX, distal-less homeobox.

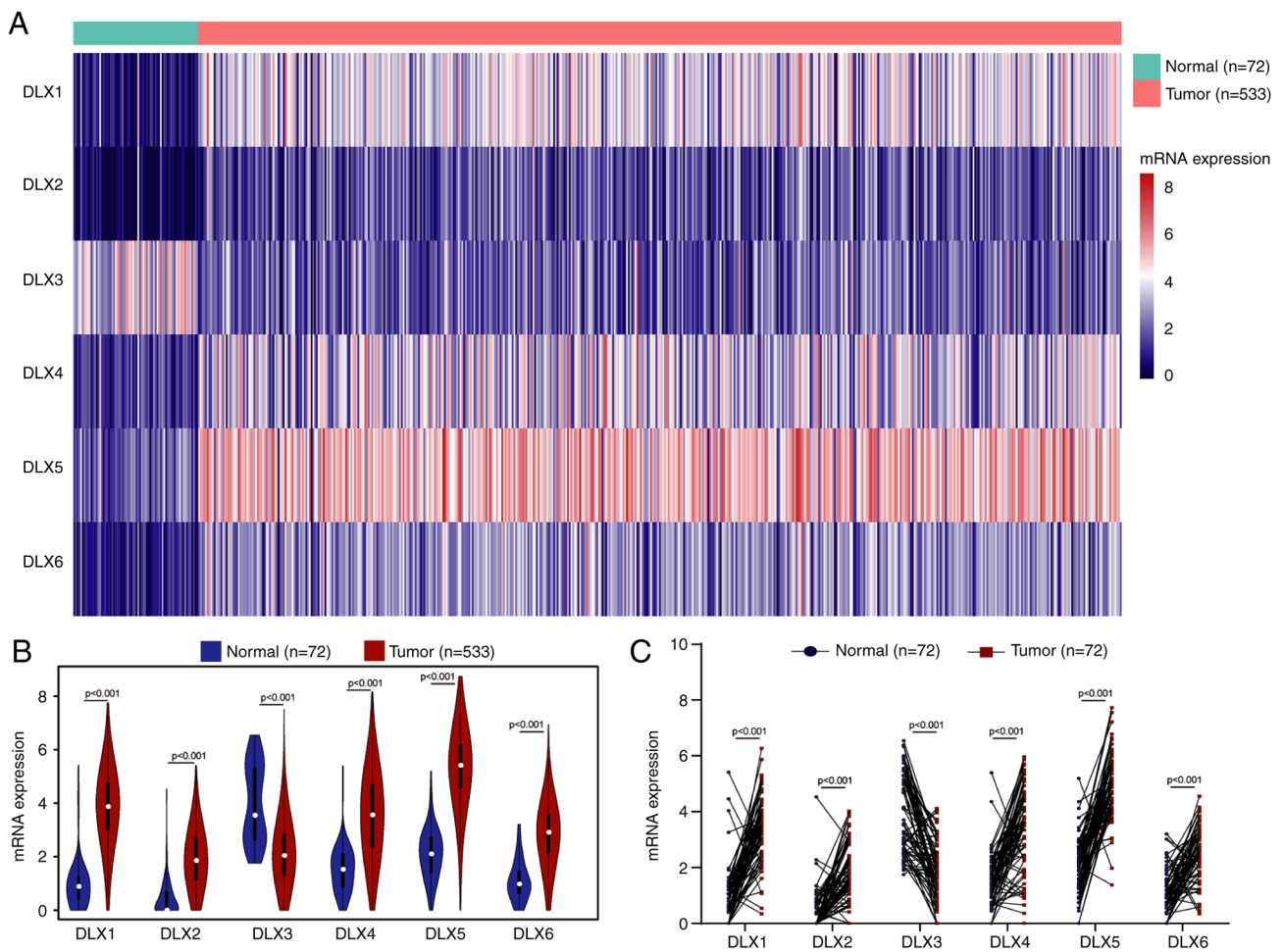


Figure 1. Expression analysis of DLX family genes in ccRCC. (A) Heat map showing the overall expression levels of six members of DLX family in TCGA database. (B) Violin plots comparing the expression levels of six members of DLX family in TCGA database. (C) Comparison of DLX gene expressions in paired ccRCC and adjacent normal renal tissue. DLX, distal-less homeobox; TCGA, The Cancer Genome Atlas; ccRCC, clear cell renal cell carcinoma.

were used to evaluate the prognostic significances of the DLX family in ccRCC. Kaplan-Meier curves for overall survival revealed poor prognosis in high DLX2 expression group (Fig. 2B), DLX4 (Fig. 2D) and DLX5 (Fig. 2E) for patients with ccRCC. However, the overall survival rates between the high and low expression group of DLX1 (Fig. 2A), DLX3 (Fig. 2C) and DLX6 (Fig. 2F) were not significantly different.

DFS was also compared between the high and low expression groups. A significantly lower DFS rate was identified in the high expression group of DLX2 (Fig. 2H), DLX4 (Fig. 2J) and DLX5 (Fig. 2K) relative to the low expression group. However, the DFS rate was not significantly different between DLX1 (Fig. 2G), DLX3 (Fig. 2I) and DLX6 (Fig. 2L). The expression of DLX2 and DLX4 was revealed to be associated with overall

Table II. Association between DLX2 or DLX4 mRNA expression and clinicopathological characteristics of patients with clear cell renal cell carcinoma.

| Clinicopathological characteristic | DLX2 mRNA expression | | | | DLX4 mRNA expression | | | |
|------------------------------------|----------------------|-------------------|----------|---------|----------------------|-------------------|----------|---------|
| | High (n=266) | Low (n=267) | χ^2 | P-value | High (n=266) | Low (n=267) | χ^2 | P-value |
| Age, years (mean \pm SD) | 60.27 \pm 12.12 | 60.98 \pm 12.18 | | 0.5 | 59.84 \pm 11.9 | 61.41 \pm 12.36 | | 0.136 |
| Sex | | | 0 | 1 | | | 18.977 | <0.001 |
| Male | 172 | 173 | | | 185 | 160 | | |
| Female | 94 | 94 | | | 81 | 107 | | |
| Stage | | | 6.97 | 0.138 | | | 41.738 | <0.001 |
| I | 124 | 143 | | | 103 | 164 | | |
| II | 24 | 33 | | | 23 | 34 | | |
| III | 69 | 54 | | | 78 | 45 | | |
| IV | 48 | 35 | | | 60 | 23 | | |
| Unknown | 1 | 2 | | | 2 | 1 | | |
| Grade | | | 2.39 | 0.664 | | | 49.563 | <0.001 |
| G1 | 7 | 7 | | | 3 | 11 | | |
| G2 | 107 | 122 | | | 87 | 142 | | |
| G3 | 109 | 97 | | | 113 | 93 | | |
| G4 | 40 | 36 | | | 61 | 15 | | |
| Unknown | 3 | 5 | | | 2 | 6 | | |
| T stage | | | 5.483 | 0.14 | | | 34.486 | <0.001 |
| T1 | 126 | 147 | | | 108 | 165 | | |
| T2 | 32 | 37 | | | 31 | 38 | | |
| T3 | 101 | 79 | | | 118 | 62 | | |
| T4 | 7 | 4 | | | 9 | 2 | | |
| N stage | | | 0.061 | 0.806 | | | 5.254 | 0.022 |
| N0/Nx | 259 | 258 | | | 253 | 264 | | |
| N1 | 7 | 9 | | | 13 | 3 | | |
| M stage | | | 1.531 | 0.216 | | | 17.329 | <0.001 |
| M0/Mx | 221 | 233 | | | 209 | 245 | | |
| M1 | 45 | 34 | | | 57 | 22 | | |

DLX, distal-less homeobox.

and DFS in ccRCC patients in both survival distribution difference assessment and Kaplan-Meier curves. Difference in either overall survival or DFS were not identified for several genes, including DLX3 and DLX5. Therefore, DLX2 and DLX4 were selected for subsequent analyses.

Association between clinicopathological characteristics and DLX2 or DLX4. To investigate the association of DLX2 and DLX4 with the distributions of clinical phenotypes, patients were divided into two subgroups according to the median mRNA expression levels. A high proportion of males, advanced pathological stage, higher grade, higher T stage, N1 stage, and M1 stage were identified in the high expression group of DLX4 (Table II); however, no significant difference was identified for age distribution (Table II). In addition, the expression of DLX2 was not shown to be associated with the clinicopathological variables examined for patients with

ccRCC (Table II). Therefore, DLX4 was selected for further studies. Univariate Cox regression analysis showed that the expression level of DLX4 was a risk factor for overall survival (Table III) and DFS (Table IV) in ccRCC patients. Based on multivariate Cox hazard analysis, the expression level of DLX4 was an independent risk variable for the overall survival of ccRCC patients (Table III) and DFS (Table IV) after integration with multiple clinicopathological characteristics. These findings indicated that the expression level of DLX4 was as an independent prognostic predictor for ccRCC patients, which may provide a supplement for clinical factors.

The relationships between clinical variables and DLX4 expression levels were investigated in the TCGA dataset. The expression levels of DLX4 were significantly higher in stage 3&4 vs. 1&2 (Fig. 3A and D), grade 3&4 vs. 1&2 (Fig. 3B and E) and T 3&4 vs. T 1&2 (Fig. 3C and F). In addition, high expression levels of DLX4 were observed

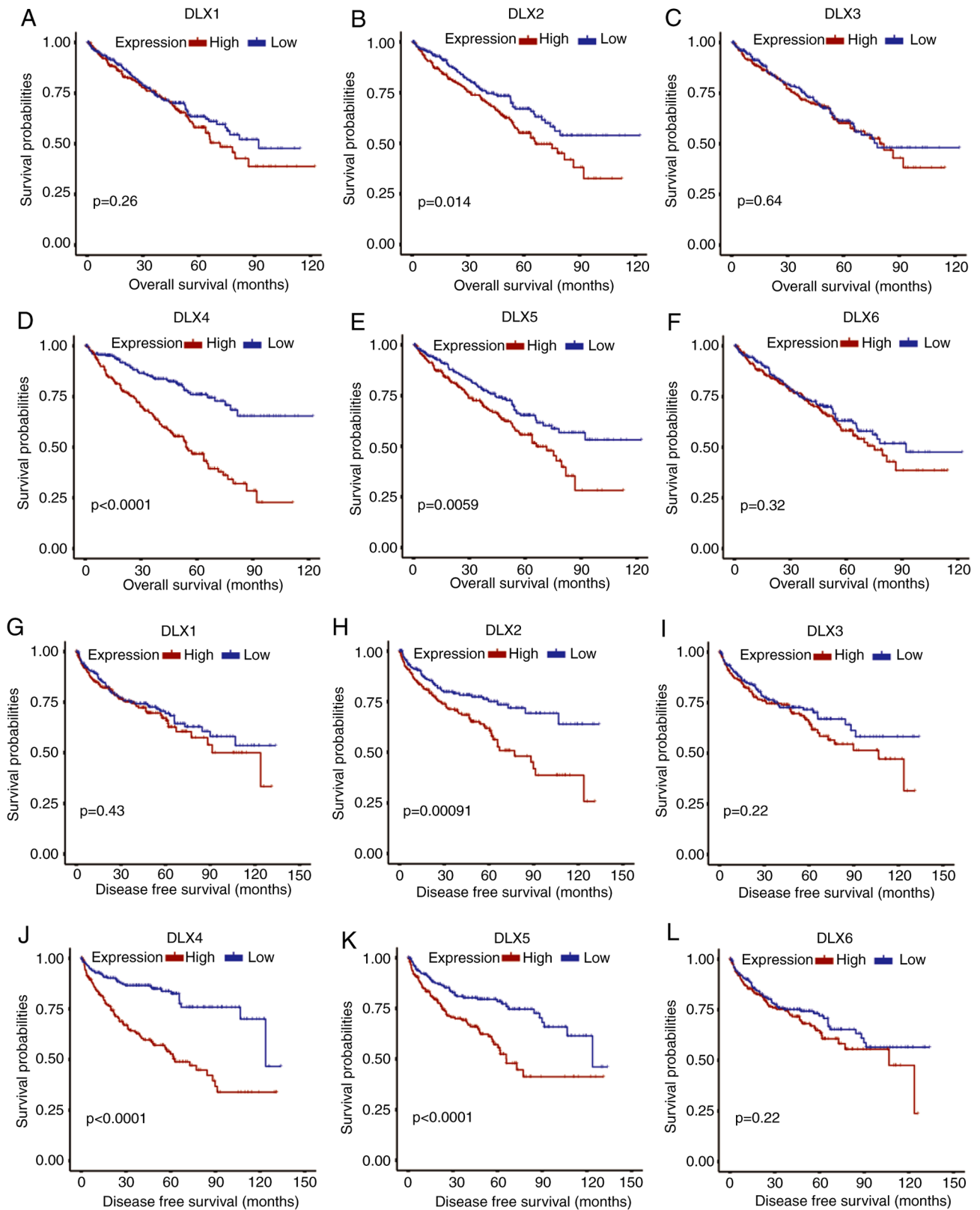


Figure 2. Prognostic values of DLX family in clear cell renal cell carcinoma. Kaplan-Meier curves of the overall survival for (A) DLX1, (B) DLX2, (C) DLX3, (D) DLX4, (E) DLX5 (F) and DLX6 (F) Kaplan-Meier curves of the disease-free survival for (G) DLX1, (H) DLX2, (I) DLX3, (J) DLX4, (K) DLX5 (L) and DLX6 (L). DLX, distal-less homeobox.

in N1 vs. N0 stage (Fig. 3G), M1 vs. M0 stage (Fig. 3H) and dead vs. alive (Fig. 3I). These results suggested that the expression levels of DLX4 were highly associated with tumor malignancy.

Diagnostic and prognostic value of DLX4 mRNA expression in ccRCC. Based on the prognostic values of DLX4 for the overall and DFS of patients with ccRCC in TCGA dataset, it was sought to further confirm the prognostic

Table III. Univariate and multivariate Cox hazard analyses of DLX4 mRNA expression levels for overall survival of patients (n=511).

| Clinicopathological characteristic | Univariate analysis | | | Multivariate analysis ^a | | |
|------------------------------------|---------------------|-------------|---------|------------------------------------|-------------|---------|
| | HR | 95% CI | P-value | HR | 95% CI | P-value |
| Age, years | 1.702 | 1.243-2.332 | <0.001 | 1.54 | 1.122-2.112 | 0.007 |
| ≤60 (n=258) | | | | | | |
| >60 (n=253) | | | | | | |
| Sex | 1.024 | 0.743-1.409 | 0.886 | | | |
| Female (n=176) | | | | | | |
| Male (n=335) | | | | | | |
| T stage | 1.839 | 1.571-2.152 | <0.001 | 1.306 | 1.083-1.576 | 0.005 |
| T1 or T2 (n=326) | | | | | | |
| T3 or T4 (n=185) | | | | | | |
| N stage | 3.579 | 1.885-6.798 | <0.001 | 1.835 | 0.952-3.537 | 0.069 |
| N0 or NX (n=497) | | | | | | |
| N1 (n=14) | | | | | | |
| M stage | 4.488 | 3.262-6.175 | <0.001 | 2.527 | 1.749-3.654 | <0.001 |
| M0 or MX (n=433) | | | | | | |
| M1 (n=78) | | | | | | |
| Grade | 1.618 | 1.357-1.929 | <0.001 | 1.241 | 1.028-1.5 | 0.025 |
| G1 or G2 (n=235) | | | | | | |
| G3 or G4 (n=276) | | | | | | |
| DLX4 expression | 2.841 | 2.027-3.982 | <0.001 | 1.885 | 1.320-2.691 | <0.001 |
| Low (n=255) | | | | | | |
| High (n=256) | | | | | | |

^aMultivariate models are adjusted for TNM classification, age, grade and DLX4 expression level. CI, confidence interval; DLX, distal-less homeobox; HR, hazard ratio.

significances of DLX4 in different subgroups of patients. A worse overall survival rate was revealed in the high DLX4 expression group compared with the low expression group for male, female, stage I and II, stage III and IV, grade 1 and grade 2, grade 3 and grade 4, low age (≤60 years) and elderly (>60 years) subgroups (Fig. 4A). In addition, a worse DFS rate was identified in high compared with low expression group for male, female, stage I and II, grade 1 and grade 2, high age (>60 years) and low age (≤60 years) subgroups (Fig. 4B). However, DFS was not significantly different between stage III and IV and grade 3 and grade 4 subgroups. These results suggested that DLX4 may be a potential prognostic biomarker for ccRCC. To determine whether the expression of DLX4 has diagnostic values in ccRCC, ROC curves were generated and AUCs were calculated to determine the diagnostic efficiency. DLX4 could sufficiently differentiate ccRCC from normal tissues with an AUC of 0.863 in the entire TCGA dataset (Fig. 4C). In addition, the diagnostic values of DLX4 expression levels were evaluated for paired normal and adjacent tumor samples in TCGA dataset, with an AUC of 0.837 (Fig. 4D). These results suggested that DLX4 may be a potential biomarker for ccRCC patients with favorable diagnostic performance.

DLX4 is highly expressed in ccRCC tissues. To further confirm the expression levels of DLX4 in ccRCC vs. normal renal tissue, RT-qPCR and immunohistochemistry were used to verify the results of the TCGA databases at the mRNA and protein levels. The results revealed higher DLX4 mRNA expression levels in ccRCC samples compared with matched normal renal samples (Fig. 5A and B). Furthermore, the expression levels of DLX4 in ccRCC samples and the matched normal renal samples were detected using immunohistochemistry, which revealed higher protein levels of DLX4 in ccRCC tissues (Fig. 5C and D). These results indicated that DLX4 was highly expressed in ccRCC tissues, which aligns with the TCGA database analysis results aforementioned.

Biological pathogenesis of DLX4 in ccRCC. To investigate the functional mechanism of DLX4 in ccRCC, genes that are highly associated with the expression levels of DLX4 in ccRCC were first selected; of which 328 positively related genes and 210 negatively associated genes were selected (Fig. 6A). Functional enrichment analysis of these genes was carried out to determine the potential mechanisms. The GO terms, including 'positive regulation of ubiquitin protein ligase activity', 'positive regulation of protein phosphorylation', 'mitotic nuclear division', 'microtubule cytoskeleton organization', and 'cell

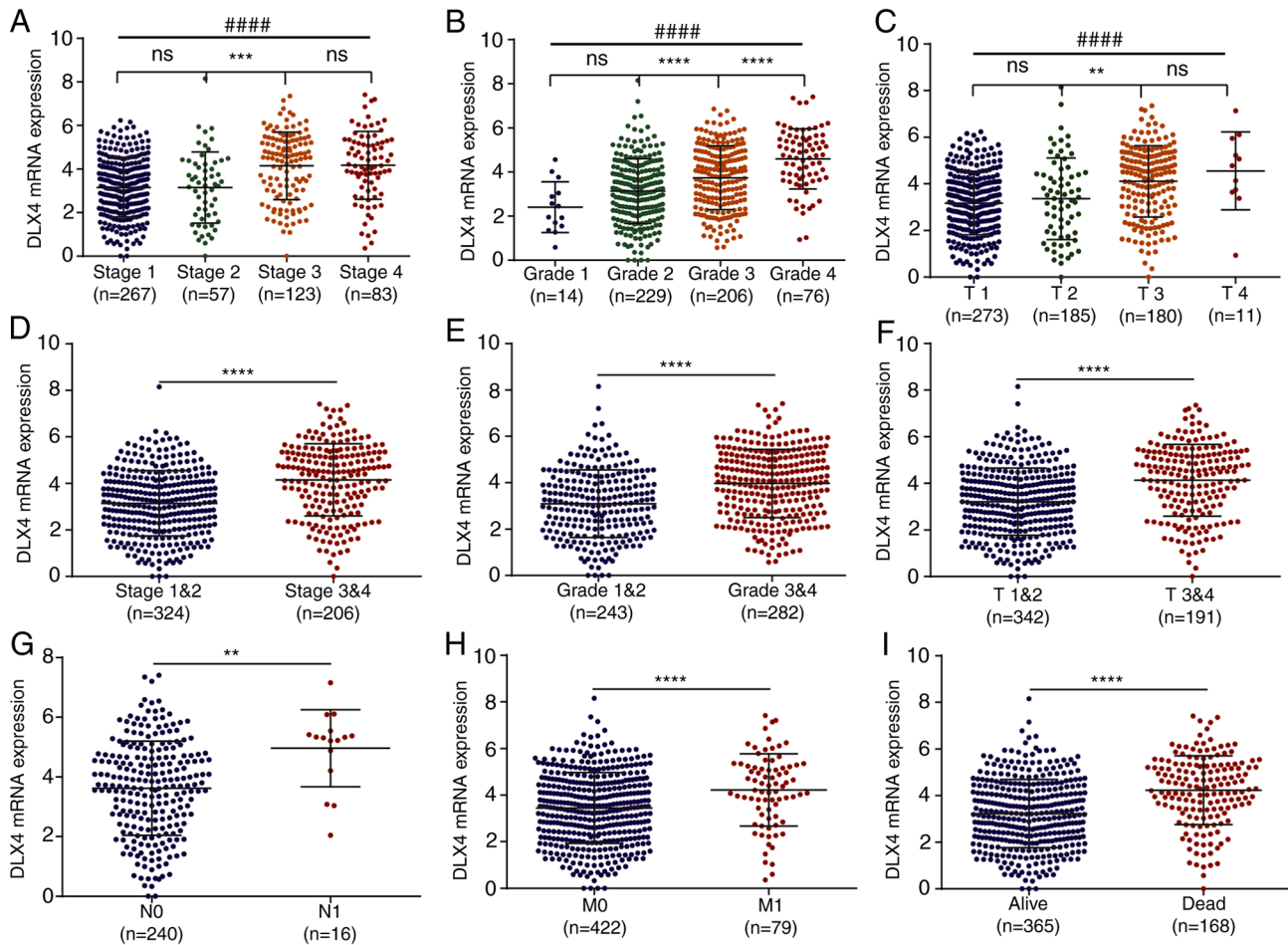


Figure 3. Association with clinicopathological variables for DLX2 and DLX4. Comparisons of the expression levels of DLX4 for different subgroups of patients from (A) pathological stage 1 to stage 4, (B) pathological grade 1 to grade 4; and (C) tumor stage T1 to T4 (C) Comparisons of the expression levels of DLX4 for patients (D) between pathological stages 1 and 2 and stages 3 and 4, (E) between pathological grades 1 and 2 and grades 3 and 4, (F) between tumor stages T1 and T2 and stages T3 and T4, (G) between lymphatic metastasis N0 and N1, (H) between distant metastasis M0 and M1, and (I) between alive and dead. ** $P < 0.01$, *** $P < 0.001$, **** $P < 0.0001$ and ##### $P < 0.0001$. DLX, distal-less homeobox; ns, not significant.

division' were enriched for biological process (Fig. 6B); 'extracellular region', 'endoplasmic reticulum lumen', 'extracellular exosome', and 'cytoplasmic microtubule' were enriched for cellular component (Fig. 6C) and 'protein domain specific binding', 'identical protein binding', 'RNA polymerase II regulatory region sequence-specific DNA binding', 'protein kinase binding', and 'enzyme binding' were enriched for molecular function (Fig. 6D). The terms 'cell cycle', 'PPAR signaling pathway' and 'fatty acid degradation' were enriched for KEGG pathways (Fig. 6E). In addition, the terms that are more closely related to the cell cycle and complement and coagulation cascades were selected and highlighted in red in Fig. 6.

Patients with ccRCC in the TCGA dataset were divided into high and low expression groups based on median expression level of DLX4. GSEA was then performed to determine the statistical significance of the biological pathways associated with the expression levels of DLX4 (Fig. 7A, C and E). The results revealed that the expression of DLX4 was associated with biological pathways related to G2M checkpoint, epithelial-mesenchymal transition (EMT), glycolysis, inflammatory response and TNF α signaling via NF- κ B. The distributions of cell cycle-related genes for high and low DLX4 expression

groups are presented in Fig. 7B. Based on the heat map, patients in the high DLX4 expression group exhibited a trend of higher expression levels of cell cycle-related genes compared with the low DLX4 expression group. Genes involved in EMT were expressed at notably higher expression levels in the high DLX4 expression group (Fig. 7D). The distributions of the inflammatory molecules, including chemokines, cytokines and their receptors, between the high and low expression groups of DLX4 were also compared (Fig. 7F). A trend towards higher expression of inflammatory molecules was identified in patients in the high DLX4 expression group. These findings suggested that cell cycle-related pathways, EMT and inflammatory response may be a potential mechanism of DLX4 in ccRCC tumorigenesis.

Immune cell infiltration associated with DLX4 expression.

Based on the associations of DLX4 expression with inflammatory and immune responses, the associations between the expression levels of DLX4 and immune cell infiltration were investigated by examining the differences in the expression profiles of 28 immune cell types separated into high and low DLX4 expression groups of DLX4 (Fig. 8A and B). Patients with high DLX4 expression in TCGA dataset had a high

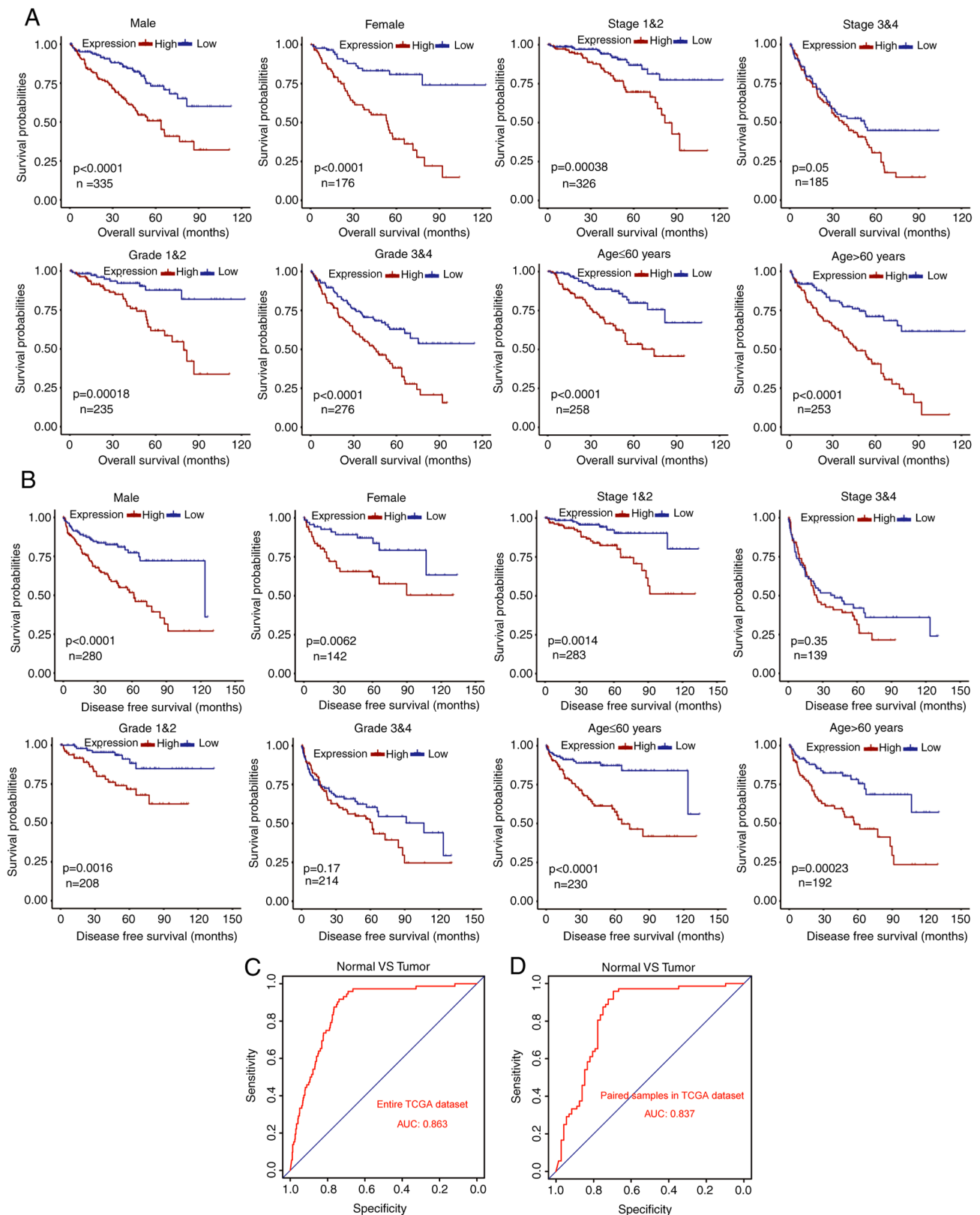


Figure 4. Prognostic values of DLX4 in different subgroups of ccRCC patients and the diagnostic value of DLX4. Kaplan-Meier curves of (A) overall survival and (B) disease-free survival of DLX4 in different subgroups of patients with ccRCC patients. Diagnostic value of DLX4 in ccRCC (C) for all samples in The Cancer Genome Atlas dataset and (D) for paired tumor and adjacent normal tissue. ccRCC, clear cell renal cell carcinoma; DLX, distal-less homeobox.

percentage of immune cells, including immature dendritic cells, activated dendritic cells, gamma delta T cells, macrophages, myeloid-derived suppressor cells (MDSCs), plasmacytoid dendritic cells, regulatory T cells and T follicular helper cells.

In addition, a positive correlation was determined between the expression levels of DLX4 and tumor immunosuppressive cells, including immature dendritic cells, activated dendritic cells, gamma delta T cells, macrophages, MDSCs, plasmacytoid

Table IV. Univariate and multivariate Cox hazard analyses of DLX4 mRNA level for DFS of patients (n=422).

| Clinicopathological characteristic | Univariate analysis | | | Multivariate analysis ^a | | |
|------------------------------------|---------------------|--------------|---------|------------------------------------|-------------|---------|
| | HR | 95% CI | P-value | HR | 95% CI | P-value |
| Age (years) | 1.366 | 0.959-1.945 | 0.084 | | | |
| ≤60 (n=230) | | | | | | |
| >60 (n=192) | | | | | | |
| Sex | 1.429 | 0.962-2.123 | 0.077 | | | |
| Female (n=142) | | | | | | |
| Male (n=280) | | | | | | |
| T stage | 4.527 | 3.134-6.539 | <0.001 | 1.396 | 1.131-1.726 | 0.002 |
| T1 or T2 (n=283) | | | | | | |
| T3 or T4 (n=139) | | | | | | |
| N stage | 5.955 | 2.990-11.861 | <0.001 | 2.729 | 1.346-5.536 | 0.005 |
| N0 or NX (n=410) | | | | | | |
| N1 (n=12) | | | | | | |
| M stage | 8.537 | 5.882-12.398 | <0.001 | 5.176 | 3.415-7.845 | <0.001 |
| M0 or MX (n=371) | | | | | | |
| M1 (n=51) | | | | | | |
| Grade | 1.832 | 1.491-2.252 | <0.001 | 2.301 | 1.306-3.157 | 0.002 |
| G1 or G2 (n=208) | | | | | | |
| G3 or G4 (n=214) | | | | | | |
| DLX4 expression | 3.011 | 2.040-4.444 | <0.001 | 1.887 | 1.245-2.860 | 0.003 |
| Low (n=211) | | | | | | |
| High (n=211) | | | | | | |

^aMultivariate models are adjusted for TNM classification, grade and DLX4 expression level. CI, confidence interval; DFS, disease-free survival; DLX, distal-less homeobox; HR, hazard ratio.

dendritic cells, regulatory T cells and T follicular helper cells (Fig. 8C). The immune and stromal scores for TCGA cohort were calculated using the ESTIMATE algorithm. Patients in the high DLX4 expression group had significantly higher immune and stromal scores compared with the low DLX4 expression group (Fig. 8D and E, respectively). Furthermore, patients in the high DLX4 expression group had significantly higher TMB and cytolytic activity scores compared with those in the DLX4 low expression group (Fig. 8F and G, respectively).

Discussion

RCC is one of the most lethal urological malignancies with high tumor heterogeneity (33); ccRCC is the most common histological subtype. Prevalence of ccRCC has steadily increased (34), placing a heavy burden on health and property of individuals. Biomarkers that could be used to accurately diagnose or predict patient prognosis are thus urgently required. In the present study, bioinformatics methods were used to explore the functions of six members of the DLX gene family in ccRCC in multiple public databases. DLX4, that may serve a more important role in patients with ccRCC. Subsequently, the diagnostic and prognostic values, the association with clinical factors and the potential functional mechanisms of DLX4

were systematically investigated. The associations between DLX4 expression and the tumor immune microenvironment were systematically evaluated.

Members of the DLX gene family contain a homeobox that could encode genes expressed in the head and limbs of the developing fruit fly. The DLX gene family includes six different members, DLX1-DLX6, and is hypothesized to serve vital roles in forebrain and craniofacial development (35). Recently, multiple studies have demonstrated different expression patterns of the DLX gene family in malignant tissues compared with non-malignant tissues (12). Several members of the DLX gene family are involved in early development and cell differentiation and are frequently dysregulated in cancer (12,13,36). At present, the roles of the DLX gene family in ccRCC remain unclear. Therefore, the present study examined the expression levels of the six members of the DLX gene family in ccRCC. Based on the results, the expression levels of the six members of the DLX gene family were different between tumor and normal tissues. These findings suggested that the DLX gene family may play vital roles in the tumorigenesis and development of ccRCC. A previous study revealed that DLX2 could counteract TGF- β induced cell cycle arrest and apoptosis to promote tumorigenesis (16). DLX2 has also been considered to be a marker of survival and disease progression in prostate cancer (17). DLX5 is involved in the growth and

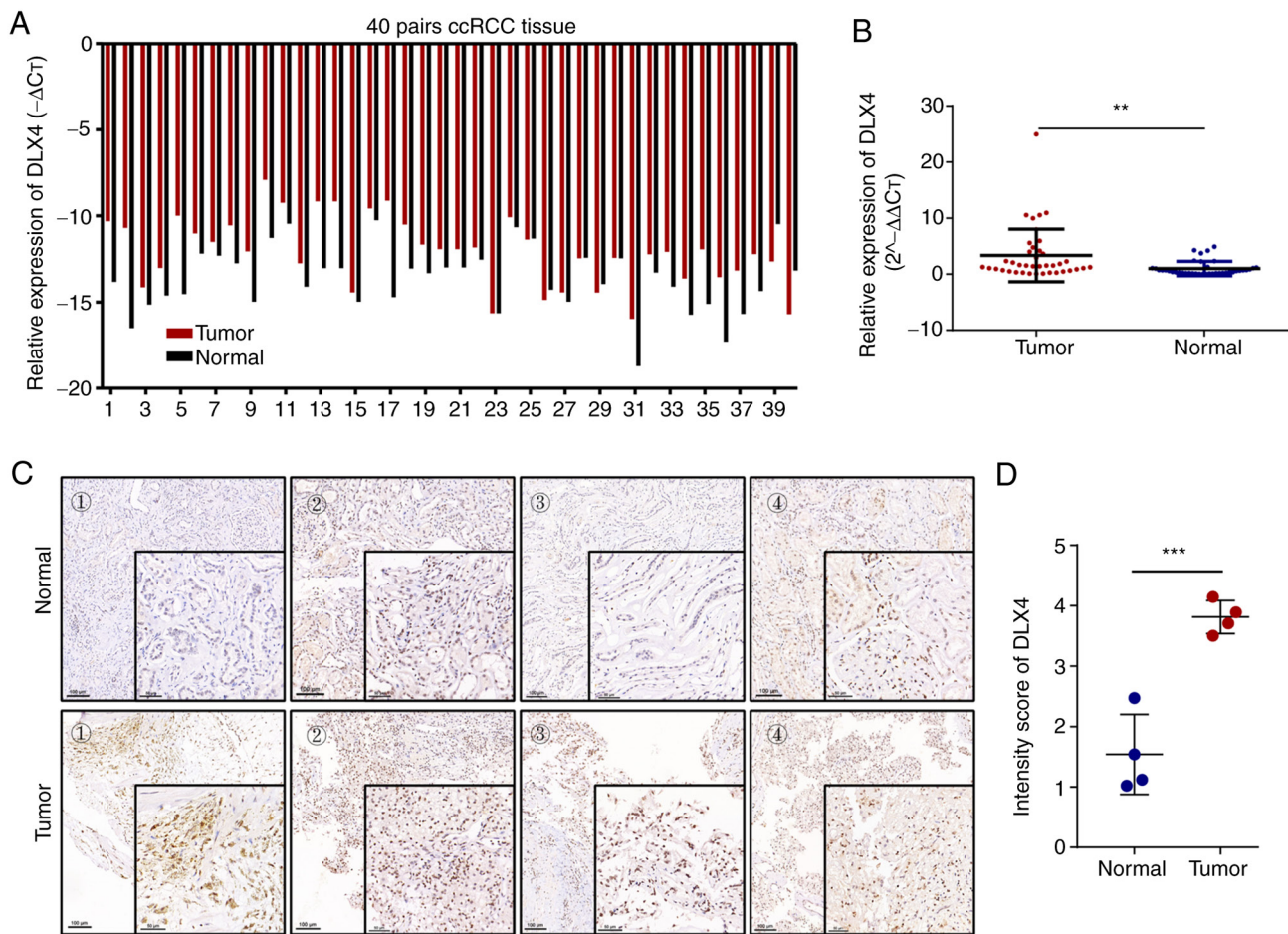


Figure 5. High expression levels of DLX4 in ccRCC tissues. (A and B) Reverse transcription-quantitative PCR revealed high expression levels of DLX4 mRNA in ccRCC tissues compared with normal adjacent tissue. (C and D) Immunohistochemistry showed high expression levels of DLX4 protein in ccRCC tissues compared with normal adjacent tissue. Scale bar for entire images and local magnification images were 100 and 50 μ m, respectively. ccRCC, clear cell renal cell carcinoma; DLX, distal-less homeobox. ** $P < 0.01$, *** $P < 0.001$.

metastasis of invasive glioma cells (19). Genes with prognostic values and those associated with clinical factors have more clinical significance. In the present study, it was demonstrated that the DLX2 and DLX4 genes have prognostic value for overall survival and DFS of patients with ccRCC, indicating their potential for use as prognostic biomarkers for ccRCC. In addition, the expression of DLX4 was revealed to be closely associated with clinical factors in ccRCC patients. However, further studies may be necessary to examine the differential expression and functional phenotype of all these genes.

DLX4 proteins, first identified in human placental tissue, is involved in the development and maturation of the placenta. The human DLX4 gene encodes three functionally different protein isoforms: β protein 1 (BP1), DLX7 and unidentified DLX4 (13). DLX7 has rarely been studied, and recent research has mainly focused on BP1; thus, BP1 is also called DLX4 (13). The expression of DLX4 in different types of cancer and the characteristics of malignant behavior have been reported. For example, high expression of DLX4 has been verified in various cancers, including leukemia, breast, prostate, liver, endometrial and ovarian, and this high expression levels may promote tumor progression (37,38). In endometrial cancer, DLX4 overexpression leads to the upregulation of genes related to proliferation, metastasis

and cell cycle to promote cell proliferation and migration, and is associated with poor prognosis (37). In inflammatory breast cancer, DLX4 promotes tumor progression, invasion and metastasis (39). In breast cancer, DLX4 drives the expression of twist to promote epithelial to mesenchymal transition, cancer migration, invasion and metastasis (40). In prostate cancer, DLX4 is an important upstream factor in the carcinogenic pathway of prostate cancer, which may contribute to tumor progression and invasion (41). In ovarian cancer, DLX4 promotes peritoneal metastasis of tumor cells by stimulating IL-1 β -mediated NF- κ B activity (21). In choriocarcinoma, DLX4 may be involved in the survival of human choriocarcinoma cells by inhibiting apoptosis (42). In the present study, the roles and potential mechanisms of DLX4 in ccRCC were investigated. A recent study showed that DLX4 contributed to the proliferation and migration of ccRCC via EMT pathways (43). The present study further extends the above research conclusions. Accordingly, DLX4 was revealed to be an independent risk factor and a potential diagnostic and prognostic biomarker for ccRCC. In the development of ccRCC, cancer-related biological pathways, including the cell cycle, EMT and immune response, were significantly altered. Cell cycle-related gene expression signatures are a marker of highly proliferative cells and, thus,

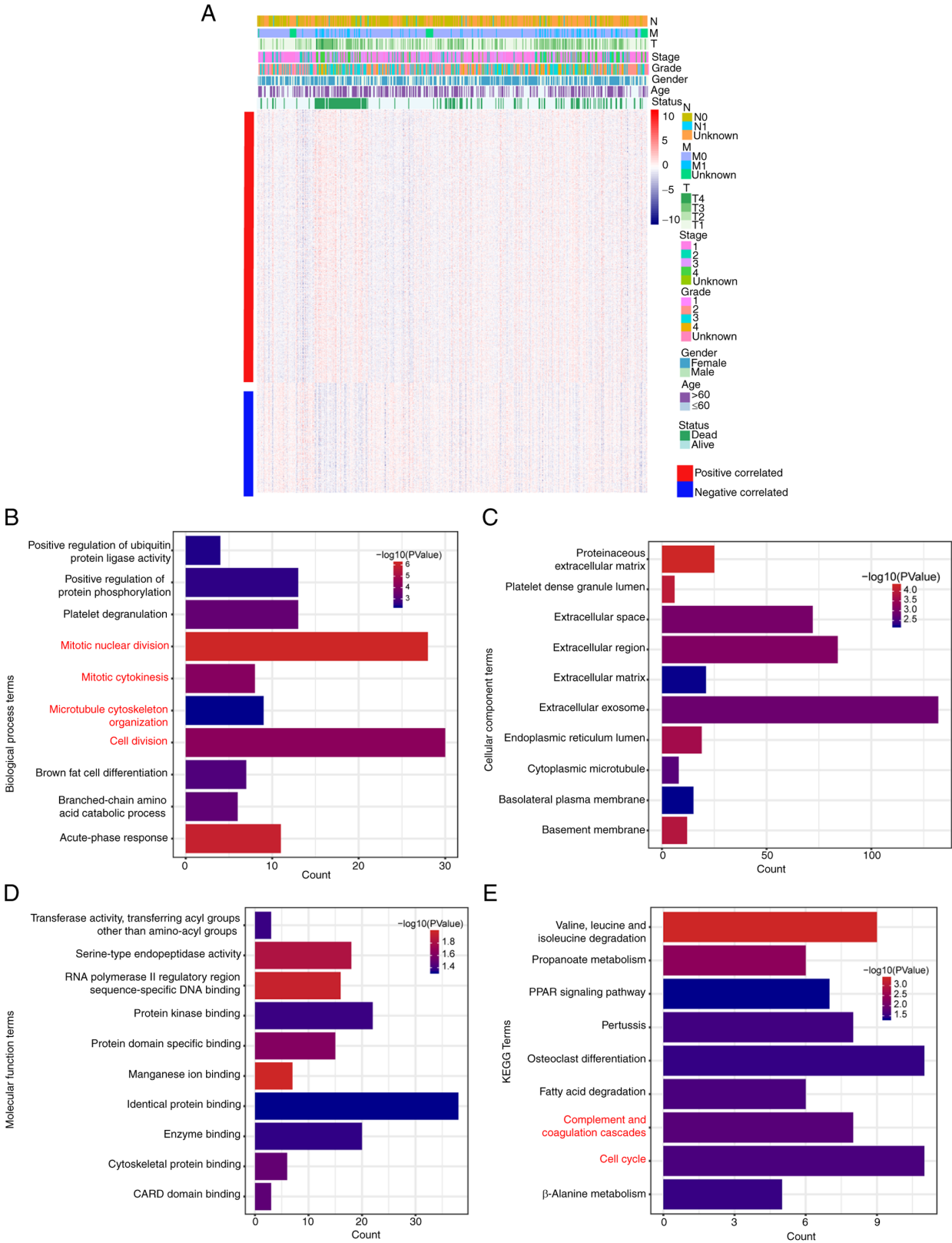


Figure 6. GO term and KEGG pathway functional enrichment analysis of DLX4 in ccRCC. (A) Heat map of genes associated with DLX4 expression (Pearson IRI>0.4), and the distribution of their clinical features. GO functional term enrichment analysis of DLX4 in ccRCC for (B) biological process, (C) cellular component, (D) molecular function. (E) KEGG pathway enrichment analysis. The terms that are closely related to the cell cycle were selected and highlighted in red. ccRCC, clear cell renal cell carcinoma; DLX, distal-less homeobox; GO, Gene Ontology; KEGG, Kyoto Encyclopedia of Genes and Genomes.

widely regarded as a biomarkers of aggressive malignancy and poor prognosis (44). In the present study, it was revealed that cell cycle-related genes were significantly higher in the

high DLX4 expression group, suggesting that DLX4 may promote tumor progression by changing the cell cycle. EMT is characterized by the loss of epithelial characteristics and/or

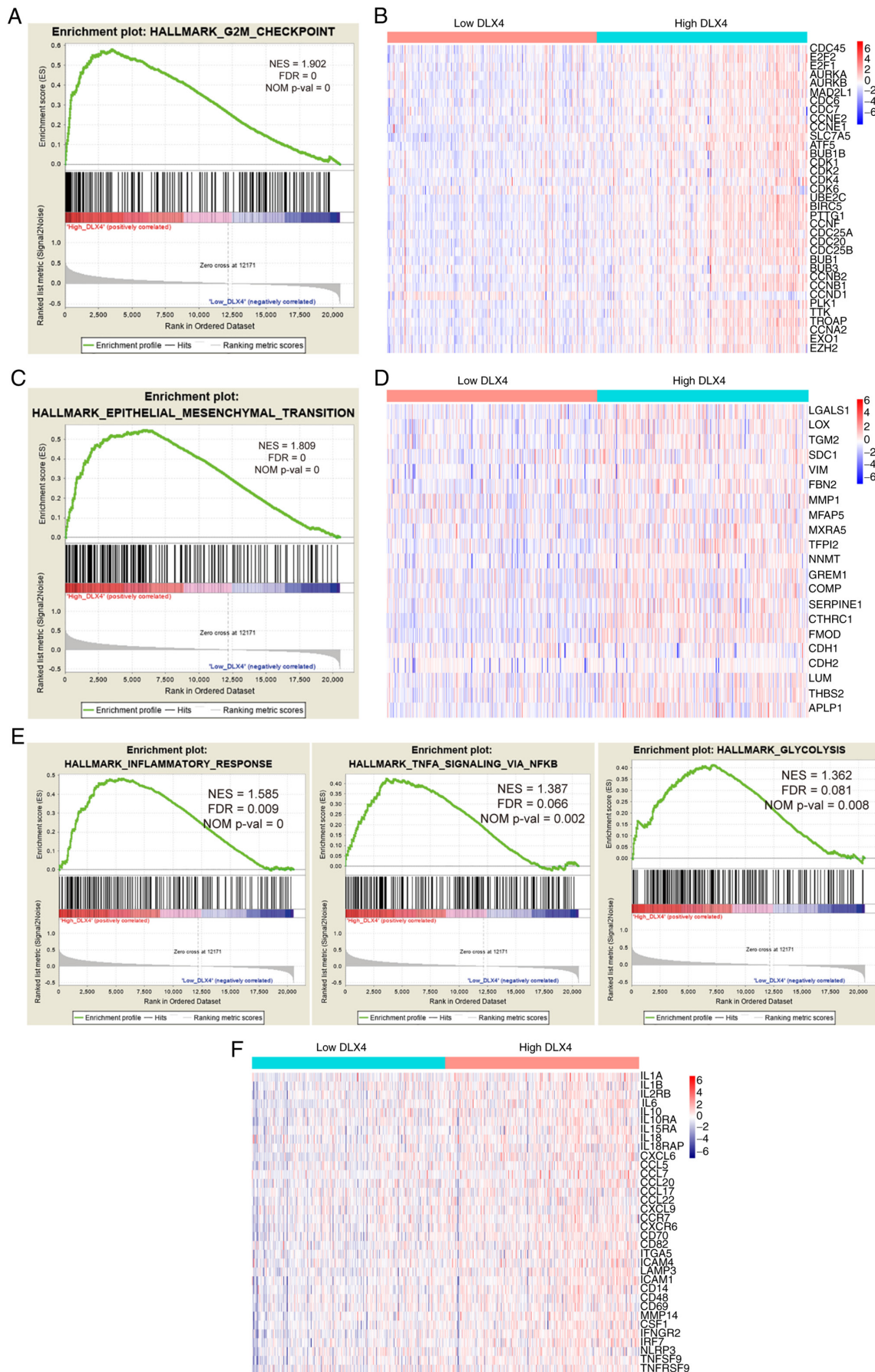


Figure 7. Gene set enrichment analysis and comparison of related pathway genes. (A and B) Enriched cell cycle pathway for DLX4 gene in The Cancer Genome Atlas dataset, and distribution patterns for genes of cell cycle. (C and D) Enriched epithelial-mesenchymal transition pathway, and distribution patterns for genes of epithelial-mesenchymal transition. (E and F) Enriched inflammation related pathways, and distribution patterns for genes of inflammatory molecules. DLX, distal-less homeobox.

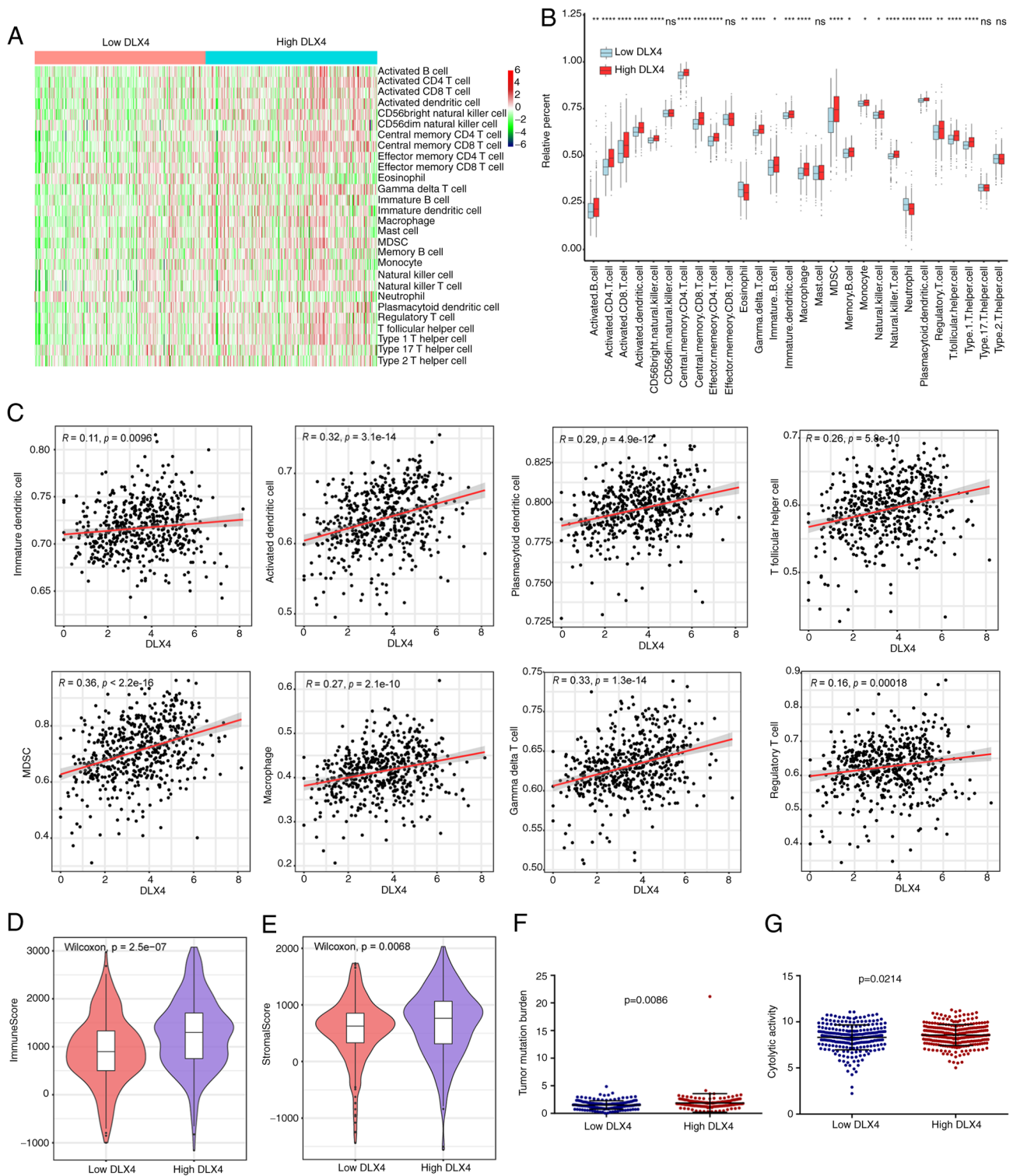


Figure 8. Association between tumor immune microenvironment and DLX4 expression. (A) The distribution patterns of 28 immune cell types in high and low DLX4 expression groups in The Cancer Genome Atlas dataset. (B) Box plots showing 28 differential immune cell infiltrations between high and low DLX4 expression groups. (C) Correlations between the expression of DLX4 and types of tumor immunosuppressive cells. The differences of (D) immune score and (E) stromal score in high and low DLX4 expression groups. The differences of (F) tumor mutation burden and (G) cytolytic activity scores in high and low DLX4 expression groups. * $P < 0.05$, ** $P < 0.01$, *** $P < 0.001$ and **** $P < 0.0001$. DLX, distal-less homeobox; MDSC, myeloid-derived suppressor cells; ns, not significant.

gain of mesenchymal characteristics, which are key components in metastasis formation (45). EMT is a highly complex biological process, and numerous factors promote and inhibit EMT. In the present study, the EMT pathway was enriched, and genes correlated with EMT exhibited increased expression levels in the high DLX4 expression group, suggesting

that DLX4 may promote tumor progression through EMT. More detailed studies are required to verify the potential functional mechanisms of DLX4 in ccRCC.

ccRCC is one of the most immune-infiltrated tumors and rapidly responds to immunotherapy (46). The level of immune cell infiltration is a key factor in determining the effect

of immunotherapy and prognosis in patients with ccRCC. Therefore, exploring the tumor immune microenvironment and identifying biomarkers associated with immunotherapeutic response have important clinical significance. Previous studies identified DLX4 as a master regulator of immune infiltration recruitment and have proposed the possibility that the expression of DLX4 may affect immune evasion in cancer (21,22). In the present study, it was revealed that immune and inflammatory pathways were significantly enriched in the high DLX4 expression group. DLX4 expression was positively correlated with the infiltration ratio of tumor immunosuppressive cells, suggesting that DLX4 may serve a role in tumor immunosuppression. These results were consistent with those that revealed that the worse prognosis of ccRCC patients was due to the tumor immune microenvironment of ccRCC being dominated by suppressed and dysfunctional cells (47). However, more detailed studies were required to verify the roles of DLX4 in the tumor immune microenvironment.

The present study found that DLX4 may be a potential diagnostic and prognostic biomarker that promotes tumor progression in ccRCC. High expression of DLX4 in ccRCC was also demonstrated and was DLX4 was revealed to be associated with the malignant characteristics of ccRCC. Furthermore, DLX4 expression was associated with the tumor immunosuppressive microenvironment. However, the present study has certain limitations. First, the associations between DLX4 and ccRCC biological behaviors must be confirmed *in vivo* and *in vitro*. Furthermore, the underlying molecular mechanisms of DLX4 facilitating ccRCC must be thoroughly investigated.

In conclusion, the present study demonstrated that high expression levels of DLX4 in ccRCC were associated with poor overall survival and DFS, as well as high tumor stage and grade. DLX4 expression was also found to be associated with the tumor immunosuppressive microenvironment. Collectively, the present data suggested that DLX4 is a promising prognostic indicator and a specific diagnostic biomarker for ccRCC. Accordingly, DLX4 may be considered a potential therapeutic target for ccRCC.

Acknowledgements

Not applicable.

Funding

No funding was received.

Availability of data and materials

The datasets used and/or analyzed during the current study are available from the corresponding author on reasonable request.

Authors' contributions

LST conceived and designed the experiments. JW and LJT acquired and analyzed the data and wrote the manuscript. YL, HL and XS collected the tissue samples and performed genetic studies. All authors read and approved the final manuscript. LJT and JW confirm the authenticity of all the raw data.

Ethics approval and consent to participate

The present study was approved by the Ethics Committee of Human Research of The Second People's Hospital of Wuhu and The First Affiliated Hospital of Anhui Medical University (approval no. PJ2019-14-22). Written informed consent was provided by all patients.

Patient consent for publication

Not applicable.

Competing interests

The authors declare that they have no competing interests.

References

1. Siegel RL, Miller KD and Jemal A: Cancer statistics, 2020. *CA Cancer J Clin* 70: 7-30, 2020.
2. Ljungberg B, Bensalah K, Canfield S, Dabestani S, Hofmann F, Hora M, Kuczyk MA, Lam T, Marconi L, Merseburger AS, *et al*: EAU guidelines on renal cell carcinoma: 2014 update. *Eur Urol* 67: 913-924, 2015.
3. Siegel RL, Miller KD and Jemal A: Cancer statistics, 2019. *CA Cancer J Clin* 69: 7-34, 2019.
4. Siegel RL, Miller KD and Jemal A: Cancer statistics, 2015. *CA Cancer J Clin* 65: 5-29, 2015.
5. Xu J, Latif S and Wei S: Metastatic renal cell carcinoma presenting as gastric polyps: A case report and review of the literature. *Int J Surg Case Rep* 3: 601-604, 2012.
6. Hsieh JJ, Purdue MP, Signoretti S, Swanton C, Albiges L, Schmidinger M, Heng DY, Larkin J and Ficarra V: Renal cell carcinoma. *Nat Rev Dis Primers* 3: 17009, 2017.
7. Ferlay J, Steliarova-Foucher E, Lortet-Tieulent J, Rosso S, Coebergh JW, Comber H, Forman D and Bray F: Cancer incidence and mortality patterns in Europe: Estimates for 40 countries in 2012. *Eur J Cancer* 49: 1374-1403, 2013.
8. Geissler K, Fornara P, Lautenschlager C, Holzhausen HJ, Seliger B and Riemann D: Immune signature of tumor infiltrating immune cells in renal cancer. *Oncoimmunology* 4: e985082, 2015.
9. Xu W, Atkins MB and McDermott DF: Checkpoint inhibitor immunotherapy in kidney cancer. *Nat Rev Urol* 17: 137-150, 2020.
10. Mantia CM and McDermott DF: Vascular endothelial growth factor and programmed death-1 pathway inhibitors in renal cell carcinoma. *Cancer* 125: 4148-4157, 2019.
11. van Oostveen J, Bijl J, Raaphorst F, Walboomers J and Meijer C: The role of homeobox genes in normal hematopoiesis and hematological malignancies. *Leukemia* 13: 1675-1690, 1999.
12. Abate-Shen C: Deregulated homeobox gene expression in cancer: Cause or consequence? *Nat Rev Cancer* 2: 777-785, 2002.
13. Lou Y, Fallah Y, Yamane K and Berg PE: BP1, a potential biomarker for breast cancer prognosis. *Biomark Med* 12: 535-545, 2018.
14. Chan DW, Hui WW, Wang JJ, Yung MM, Hui LM, Qin Y, Liang RR, Leung TH, Xu D, Chan KK, *et al*: DLX1 acts as a crucial target of FOXM1 to promote ovarian cancer aggressiveness by enhancing TGF- β /SMAD4 signaling. *Oncogene* 36: 1404-1416, 2017.
15. Sun B, Fan Y, Yang A, Liang L and Cao J: MicroRNA-539 functions as a tumour suppressor in prostate cancer via the TGF- β /Smad4 signalling pathway by down-regulating DLX1. *J Cell Mol Med* 23: 5934-5948, 2019.
16. Yilmaz M, Maass D, Tiwari N, Waldmeier L, Schmidt P, Lehembre F and Christofori G: Transcription factor Dlx2 protects from TGF β -induced cell-cycle arrest and apoptosis. *EMBO J* 30: 4489-4499, 2011.
17. Green WJ, Ball G, Hulman G, Johnson C, Van Schalwyk G, Ratan HL, Soria D, Garibaldi JM, Parkinson R, Hulman J, *et al*: KL167 and DLX2 predict increased risk of metastasis formation in prostate cancer-a targeted molecular approach. *Br J Cancer* 115: 236-242, 2016.

18. Palazzo E, Kellett M, Cataisson C, Gormley A, Bible PW, Pietroni V, Radoja N, Hwang J, Blumenberg M, Yuspa SH and Morasso MI: The homeoprotein DLX3 and tumor suppressor p53 co-regulate cell cycle progression and squamous tumor growth. *Oncogene* 35: 3114-3124, 2016.
19. Hu B, Wang Q, Wang YA, Hua S, Sauvé CG, Ong D, Lan ZD, Chang Q, Ho YW, Monasterio MM, *et al*: Epigenetic activation of WNT5A drives glioblastoma stem cell differentiation and invasive growth. *Cell* 167: 1281-1295.e18, 2016.
20. Trinh BQ, Barengo N, Kim SB, Lee JS, Zweidler-McKay PA and Naora H: The homeobox gene DLX4 regulates erythro-megakaryocytic differentiation by stimulating IL-1 β and NF- κ B signaling. *J Cell Sci* 128: 3055-3067, 2015.
21. Hara D, Trinh BQ, Ko SY, Barengo N, Liu J and Naora H: The homeoprotein DLX4 stimulates NF- κ B activation and CD44-mediated tumor-mesothelial cell interactions in ovarian cancer. *Am J Pathol* 185: 2298-2308, 2015.
22. Chen J, Cerise J, Jabbari A, Clynes R and Christiano A: Master regulators of infiltrate recruitment in autoimmune disease identified through network-based molecular deconvolution. *Cell Syst* 1: 326-337, 2015.
23. Hinrichs AS, Raney BJ, Speir ML, Rhead B, Casper J, Karolchik D, Kuhn RM, Rosenbloom KR, Zweig AS, Haussler D and Kent WJ: UCSC data integrator and variant annotation integrator. *Bioinformatics* 32:1430-1432, 2016.
24. Sing T, Sander O, Beerenwinkel N and Lengauer T: ROCr: Visualizing classifier performance in R. *Bioinformatics* 21: 3940-3941, 2005.
25. Livak KJ and Schmittgen TD: Analysis of relative gene expression data using real-time quantitative PCR and the 2(-Delta Delta C(T)) method. *Methods* 25: 402-408, 2001.
26. Qu Y, Zhao R, Zhang H, Zhou Q, Xu F, Zhang X, Xu W, Shao N, Zhou S, Dai B, *et al*: Inactivation of the AMPK-GATA3-ECHS1 pathway induces fatty acid synthesis that promotes clear cell renal cell carcinoma growth. *Cancer Res* 80: 319-333, 2020.
27. Subramanian A, Tamayo P, Mootha VK, Mukherjee S, Ebert BL, Gillette MA, Paulovich A, Pomeroy SL, Golub TR, Lander ES and Mesirov JP: Gene set enrichment analysis: A knowledge-based approach for interpreting genome-wide expression profiles. *Proc Natl Acad Sci USA* 102: 15545-15550, 2005.
28. Ge S, Hua X, Chen J, Xiao H, Zhang L, Zhou J, Liang C and Tai S: Identification of a costimulatory molecule-related signature for predicting prognostic risk in prostate cancer. *Front Genet* 12: 666300, 2021.
29. Charoentong P, Finotello F, Angelova M, Mayer C, Efremova M, Rieder D, Hackl H and Trajanoski Z: Pan-cancer immunogenomic analyses reveal genotype-immunophenotype relationships and predictors of response to checkpoint blockade. *Cell Rep* 18: 248-262, 2017.
30. Yoshihara K, Shahmoradgoli M, Martinez E, Vegesna R, Kim H, Torres-Garcia W, Trevino V, Shen H, Laird PW, Levine DA, *et al*: Inferring tumour purity and stromal and immune cell admixture from expression data. *Nat Commun* 4: 2612, 2013.
31. Chalmers ZR, Connelly CF, Fabrizio D, Gay L, Ali SM, Ennis R, Schrock A, Campbell B, Shlien A, Chmielecki J, *et al*: Analysis of 100,000 human cancer genomes reveals the landscape of tumor mutational burden. *Genome Med* 9: 34, 2017.
32. Abida W, Cheng ML, Armenia J, Middha S, Autio KA, Vargas HA, Rathkopf D, Morris MJ, Danila DC, Slovin SF, *et al*: Analysis of the prevalence of microsatellite instability in prostate cancer and response to immune checkpoint blockade. *JAMA Oncol* 5: 471-478, 2019.
33. Znaor A, Lortet-Tieulent J, Laversanne M, Jemal A and Bray F: International variations and trends in renal cell carcinoma incidence and mortality. *Eur Urol* 67: 519-530, 2015.
34. Leibovich BC, Lohse CM, Crispen PL, Boorjian SA, Thompson RH, Blute ML and Cheville JC: Histological subtype is an independent predictor of outcome for patients with renal cell carcinoma. *J Urol* 183: 1309-1315, 2010.
35. Panganiban G and Rubenstein JL: Developmental functions of the Distal-less/Dlx homeobox genes. *Development* 129: 4371-4386, 2002.
36. Popovici C, Leveugle M, Birnbaum D and Coulier F: Homeobox gene clusters and the human paralogy map. *FEBS Lett* 491: 237-242, 2001.
37. Zhang L, Wan Y, Jiang Y, Zhang Z, Shu S, Cheng W and Lang J: Overexpression of BP1, an isoform of Homeobox Gene DLX4, promotes cell proliferation, migration and predicts poor prognosis in endometrial cancer. *Gene* 707: 216-223, 2019.
38. Yu M, Yang Y, Shi Y, Wang D, Wei X, Zhang N and Niu R: Expression level of beta protein 1 mRNA in Chinese breast cancer patients: A potential molecular marker for poor prognosis. *Cancer Sci* 99: 173-178, 2008.
39. Man YG, Schwartz A, Levine PH, Teal C and Berg PE: BP1, a putative signature marker for inflammatory breast cancer and tumor aggressiveness. *Cancer Biomark* 5: 9-17, 2009.
40. Zhang L, Yang M, Gan L, He T, Xiao X, Stewart MD, Liu X, Yang L, Zhang T, Zhao Y and Fu J: DLX4 upregulates TWIST and enhances tumor migration, invasion and metastasis. *Int J Biol Sci* 8: 1178-1187, 2012.
41. Schwartz AM, Man YG, Rezaei MK, Simmens SJ and Berg PE: BP1, a homeoprotein, is significantly expressed in prostate adenocarcinoma and is concordant with prostatic intraepithelial neoplasia. *Mod Pathol* 22: 1-6, 2009.
42. Sun Y, Lu X, Yin L, Zhao F and Feng Y: Inhibition of DLX4 promotes apoptosis in choriocarcinoma cell lines. *Placenta* 27: 375-383, 2006.
43. Sun G, Ge Y, Zhang Y, Yan L, Wu X, Ouyang W, Wang Z, Ding B, Zhang Y, Long G, *et al*: Transcription factors BARX1 and DLX4 contribute to progression of clear cell renal cell carcinoma via promoting proliferation and epithelial-mesenchymal transition. *Front Mol Biosci* 8: 626328, 2021.
44. Otto T and Sicinski P: Cell cycle proteins as promising targets in cancer therapy. *Nat Rev Cancer* 17: 93-115, 2017.
45. Pallasch F and Schumacher U: Angiotensin Inhibition, TGF- β and EMT in cancer. *Cancers* 12: 2785, 2020.
46. Şenbabaoğlu Y, Gejman RS, Winer AG, Liu M, Van Allen EM, de Velasco G, Miao D, Ostrovskaya I, Drill E, Luna A, *et al*: Tumor immune microenvironment characterization in clear cell renal cell carcinoma identifies prognostic and immunotherapeutically relevant messenger RNA signatures. *Genome Biol* 17: 231, 2016.
47. Vuong L, Kotecha R, Voss M and Hakimi A: Tumor Microenvironment dynamics in clear-cell renal cell carcinoma. *Cancer Discov* 9: 1349-1357, 2019.



This work is licensed under a Creative Commons Attribution-NonCommercial-NoDerivatives 4.0 International (CC BY-NC-ND 4.0) License.